ADVANCED FUNCTIONAL MATERIALS
www.afm-journal.de

Replacing Copper Wires with Carbon Nanotube Wires in Electrical Transformers

*Lukasz Kurzepa, Agnieszka Lekawa-Raus, Jeff Patmore, and Krzysztof Koziol**

Carbon nanotubes, with their unique physical properties, have the potential to outperform conventionally used electrical wiring metals. Any improvement in this area of technology would be of great importance to industry, the economy, and the environment, as the global need for electrical energy and its efficient transfer and conversion rapidly increases. Carbon nanotube fibers, which are assemblies made purely of carbon nanotubes, can uniquely be used in macroscopic electrical applications including electrical wires and devices where the operation is enabled by these conductors. This paper presents details of the working prototype of an electrical machine, a transformer, where conventional copper wires have been replaced with conducting wires made purely of carbon nanotube fibers.

1. Introduction

The weight and power losses in electrical machines are challenging problems in many areas of current technology. For example, the transformers used in airplanes are engineered to work at a frequency of 400 Hz so as to decrease the size of the core and amount of windings, so allowing a decrease in weight.[1] However, the increase in operating frequency is directly related to higher losses in the windings as a result of both skin and proximity effects as well as the increased losses in the core.

Carbon nanotubes (CNTs) have the potential to become the next generation of highly conductive electrical wires,[2] with additional benefits of low weight, high mechanical performance,[3] little skin effect[4,5] and low costs. In this paper, we present the first working transformer that does not use any metal windings but instead relies upon conductors made entirely of carbon nanotubes. We also show that CNT wires can work successfully across a wide range of frequencies.

The development of carbon nanotube electrical wires opened up the possibility of using individual CNTs in macro applications. These wires are made of carbon nanotube fibres, that is, a network of axially aligned carbon nanotubes, which can be assembled into different diameter cords with a suitable electrical insulation applied to its surface (**Figure 1**).[2] Carbon nanotube fibres can be produced via different processes as reported by many authors[6] but for this work the floating catalyst chemical vapor deposition (CVD) process was used.[3] The individual manufactured CNT fibres have diameter of 10–20 μm and practically no limit in length.[3] The production process is very fast: the CNT synthesis takes fraction of a second and these fibres may be spun directly from the synthesis zone at the rate of 5–100 m min^{-1}. Production costs are similar to those for the production of carbon black, as CNT fibres are about 10 times less dense than copper the production cost may quickly become competitive, assuming mass production techniques. The specific electrical conductivity, that is, conductivity divided by density[7] of CNT fibre ranges from 0.2–2 × 10^6 S m^{-1} g^{-1} cm^3 at room conditions where the upper limit was recorded for recently developed CNT fibre comprising solely metallic single wall CNTs.[2,8] Further improvement of electrical conductivity may be obtained via the incremental increase of the length of CNTs, decrease of the numbers of distortions of individual CNTs and impurities, as well as precise control over the condensation and alignment of the CNTs within the fibre.

At the time of writing this paper, the precise control of the morphology of CNT fibres requires further research; however, as reported by others in the field, the specific conductivity of presently produced CNT fibres can be higher than for metals when these fibres are strongly doped with various compounds.[9,10]

Theoretically, the AC conductivity of CNT fibres should involve little skin effect across a very wide range of frequencies. Moreover, the specific mechanical strength of CNT fibres is already higher than steel, and significantly higher than copper.[2,3] The fibres are also characterized by high pliability and very high axial thermal conductivity.[11]

The successful development of a method for insulating the CNT fibres that does not compromise the conductivity through the porous structure of the fibre but forms a continuous thin layer on its surface has allowed the formation of CNT wires.[2] Such CNT wires may be used as conventional metal electrical conductors and may be easily introduced into already existing electrical circuits. Depending on the application the low resistance electrical connections between metal and CNT wire may be provided using a newly developed low temperature carbon solder,[12] a connecting paste based on silver or simple physical crimping.

L. Kurzepa, Dr. A. Lekawa-Raus, Dr. K. Koziol
Department of Materials Science and Metallurgy
University of Cambridge, Cambridge, CB2 3QZ, UK
E-mail: kk292@cam.ac.uk
J. Patmore
Pembroke College, Trumpington Street
Cambridge, CB2 1RF, UK

DOI: 10.1002/adfm.201302497

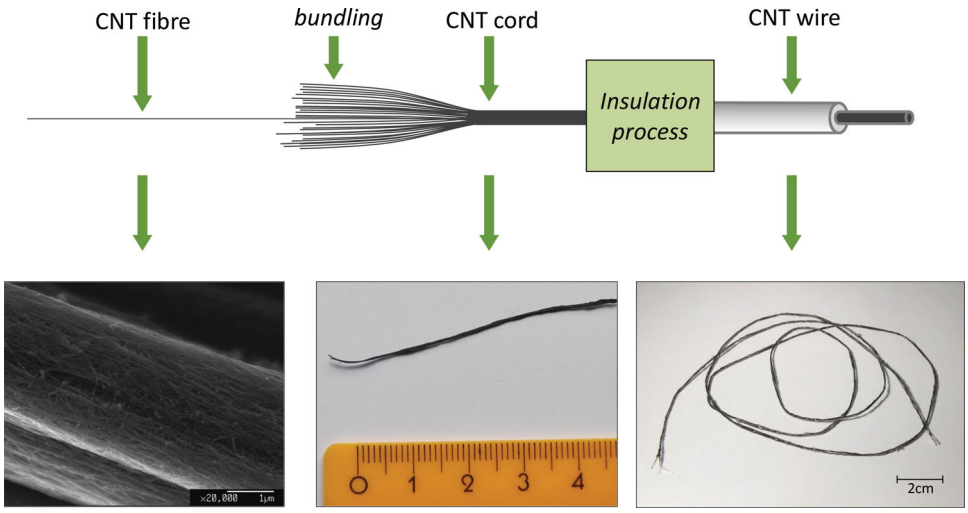

Figure 1. The process of production of CNT wire. Top left: The individual 10–20 µm thick CNT fibres are bundled together to form a CNT cord (top middle) which is later insulated with a non-conductive polymeric compound (top right). Down left: Scanning electron microscope image of the internal structure of the CNT fibre which is an assembly of axially aligned CNTs. Down middle: a photo of a cord of about 0.7 mm in diameter. Down right: a photo of about 30 cm long CNT wire, that is, insulated CNT cord.

2. Transformer Construction

One of the important areas of application of these electrical wires is in common devices such as coils, motors, and transformers. Theoretically the good performance of the wires in such devices should ensure a more efficient operation. It was therefore decided to test the performance of CNT wires in a common device, the transformer.

The windings of the transformer examined in this paper were made of CNT wires prepared from CNT cords described in the introduction, insulated with a silicone paste.[13]

The primary winding comprised 21 turns, and the secondary winding 12 turns. The primary and secondary CNT coils were placed alongside each other on the central column of a core. The core was made of two classical E-shaped elements, joined tightly with a minimal air gap,[14] as shown in **Figure 2**a.

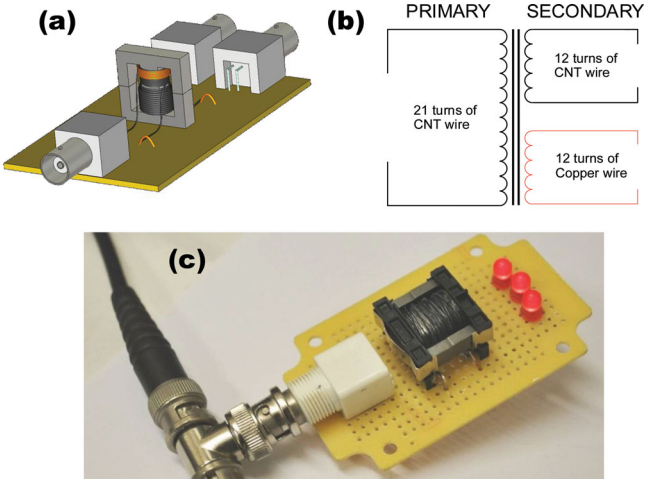

Figure 2. a) Drawing of CNT transformer, b) schematic diagram of the windings, and c) an image of the operating device.

For comparative testing, there was also an additional secondary coil made of 12 turns of copper wire which was wound on top of the secondary CNT coil. The transformer is shown schematically in Figure 2b. The optimum frequency range for the core used in this experiment is 25–500 kHz. Above 500 kHz the losses in the core increase significantly. However, as the real part of complex magnetic permeability is almost constant up to 1 MHz, in our experiments, the transformer was tested up to 1 MHz. The image of the operating transformer is shown in Figure 2c.

3. Testing of the Transformer

The characteristics of the transformer presented in **Figure 3** were recorded in an open circuit and show peak to peak (p–p) output voltages plotted against frequency. The output voltages were induced as a response to the excitation caused by current of 10 mA (p–p) applied to the primary winding of the transformer in frequency range of 1–100 kHz. The results obtained are in agreement with a classic theory of transformers. As expected, the measured characteristics are perfectly linear and are not dependent on the material used for the winding.

According the standard theory of transformers an input alternating current $\boldsymbol{I}_1$ (bold denotes a complex number) flowing in primary winding will induce magnetic flux in the core of the machine. The magnitude of the flux will be dependent on the amplitude of current, number of turns in primary coil and parameters of the core. The changing magnetic flux induces the electromotive force $\boldsymbol{E}_1$ on the primary winding and electromotive force $\boldsymbol{E}_1$ on the secondary winding whose magnitudes depend on the magnitude of the flux, frequency and number of turns in the respective coils. Thus the ratio of turns between primary N_1 and secondary N_2 winding is directly proportional to the ratio of the respective electromotive forces $\boldsymbol{E}_1$ and $\boldsymbol{E}_2$:

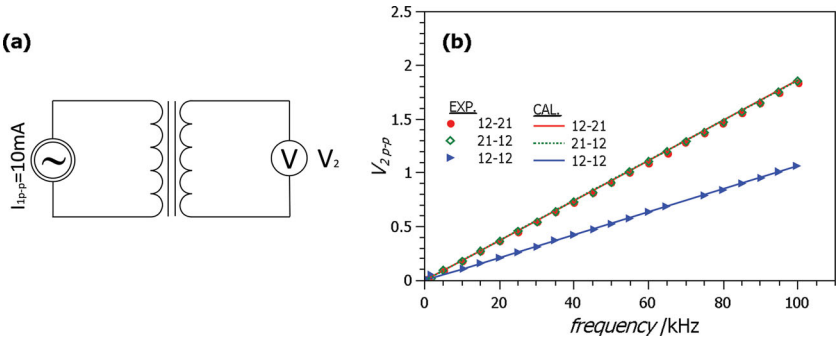

Figure 3. a) The setup used for measurements presented in (b). b) Open circuit characteristics showing output voltage V_2 as a function of frequency. The input current of $I_{1p\text{-}p}$ = 10 mA was applied to primary windings at increasing frequencies. The data points were recorded in the experiment and the lines present the results of the theoretical calculations. The arrangements of the windings used are described by the numbers in the legends. The first and second values (before and after hyphen) stand for the number of turns in the primary winding and secondary winding respectively. 21 turn coil was made of CNT wire and the 12-turn coils were either made of CNT or copper wires. As the results for latter coils were identical only the data for 12 CNT coil are presented.

$$\frac{\mathbf{E_1}}{\mathbf{E_2}} = \frac{N_1}{N_2} \tag{1}$$

In an ideal lossless transformer, that is, in which there is no drop of voltage on the resistance of the windings and no leakage inductance the primary e.m.f. will equal voltage $\boldsymbol{V_1}$ supplied to the primary winding and $\boldsymbol{E_2}$ will equal the voltage $\boldsymbol{V_2}$ on the load attached to the secondary windings. Hence the ratio of $\boldsymbol{V_1}/\boldsymbol{V_2}$ will also equal the turns ratio.

However, in any real life transformer:

$$\mathbf{V}_1 = (R_1 + \mathrm{j}\omega L_{L1})\mathbf{I}_1 + \mathbf{E}_1 \tag{2}$$

$$\mathbf{E}_2 = (R_2 + \mathrm{j}\omega L_{L2})\mathbf{I}_2 + \mathbf{V}_2 \tag{3}$$

where R_1 and R_2 are the resistances of the primary and secondary winding respectively. L_{L1} and L_{L2} stand for leakage inductances from primary and secondary windings respectively. Finally, $\boldsymbol{I_2}$ is the current on the secondary side of the transformer, j is the imaginary number, and ω is an angular frequency defined as $\omega = 2\pi f$, where f is the frequency of the supplied signal.

In the experiment presented in Figure 3b the losses, although exist, do not need to be taken into account due to two reasons. Firstly, in the open circuit conditions there is negligible current flowing in the secondary winding and the voltage measured on the secondary side of the transformer will be the secondary electromotive force $\boldsymbol{V_1} = \boldsymbol{E_2}$. Secondly, the amplitude of the input current is kept constant and it may be assumed that the current supplying core losses is negligible. Therefore, practically all the supplied current will be used to induce $\boldsymbol{E_1}$, and $\boldsymbol{E_1}$ will depend only on the frequency, number of turns of the primary windings and the parameters of the core independently of R_1, L_{L1} and core losses. Thus:

$$E_1 = 2\pi f L_1 I_1 \tag{4}$$

where L_1 is the inductance of the primary winding dependent on the number of turns and parameters of the core. L_1 may be calculated based on the inductance factor A_L (the reciprocal of the reluctance of the core, measured in the units of nH) provided by the manufacturer $-L_1 = A_L{*}N_1^2/10^9$.[14] As for our core the A_L amounts to 1470 + 30/–20%. Taking the smallest value of A_L (1470 –20%) the L_1 for 12 turns coils amounts to 0.00017 H and L_2 = 0.00052 H for 21 turns coil. Calculating the set of E_1 values from Equation 4 for constant peak to peak value of current $I_{1(p\text{-}p)}$ = 10 mA, changing frequencies and using Equation 1, the values of output voltage E_2 were obtained.[15] The calculated values of E_2 are represented by solid lines (Figure 3b). These results are in perfect agreement with the experimentally measured values (data points).

The correctness of the results is also confirmed by the fact that the characteristics of 21 turn coil used as primary winding and 12 turn coils used as secondary winding is identical to the one recorded with inverse arrangement of the coils (12 turns as primary and 21 turns as secondary). This overlapping of the characteristics results from the fact that for set value of current the E_1 induced on 12 turns coil used as primary winding is smaller than the one induced on 21 turns coil and then gets respectively increased/decreased when 21 turns coil and 12 turns coils are used as secondary windings respectively which results in the same values of E_2.

This test indicates that CNT windings function exactly as expected across the range of applied frequencies and no difference was observed between copper and CNT windings.

The next experiment was also performed in open circuit conditions. To obtain the characteristics presented in **Figure 4**a the copper coil was set as primary winding and both CNT coils were used as secondary windings. A voltage of 150 mV p–p was applied to the primary side in frequency range of 1 kHz–1 MHz and the output voltages induced in the CNT coils were recorded (Figure 4d). The characteristics show that the output voltage is independent of the frequency which is in agreement with theory and would be observed for a transformer with conventional winding. Considering the resistance of input copper winding and leakage inductance L_{L1} as negligible (which is often assumed in conventional transformers) it may be assumed that $\boldsymbol{E_1} \approx \boldsymbol{E_1}$. Thus, the constant amplitude of input voltage will result in the constant amplitude of electromotive force on the input coil and constant electromotive force on the output coil. Additionally, as indicated previously in open circuit conditions $\boldsymbol{E_2} \approx \boldsymbol{V_2}$ and no losses in the secondary winding need to be considered. Hence, as expected from Equation 1, the calculations of turns and voltage ratios give comparable results. From the characteristics presented in Figure 4a the output voltage induced in 12-turns CNT represents 150 mV p–p across the frequency range which gives exactly the voltage ratio expected. Equally when the primary to secondary turns ratio was 1.75 the average voltage recorded on the output was 257 mV a voltage ratio of 1.71. The correlation, allowing for physical construction of the transformer, with its theoretical performance is very good.

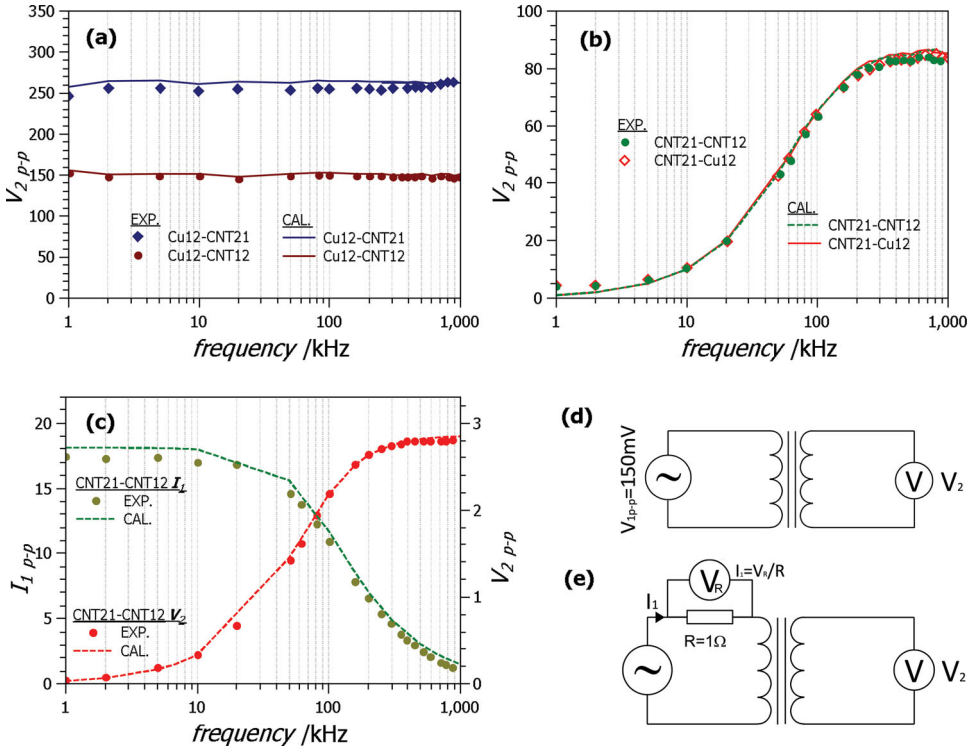

Figure 4. Open circuit characteristics showing output voltage induced in response to the input voltage of 150 mVp-p applied to primary windings at increasing frequencies versus frequency. (In all the graphs, the data points were recorded during the experiments and the lines are the results of the theoretical calculations.) a) 12-turns copper coil was used as primary winding (Cu12) and CNT coils were used as secondary windings (CNT21 and CNT12 standing for CNT coil with 21 and 12 turns respectively). b) 21-turns CNT coil was used as primary winding and 12-turns coils were used as secondary windings. c) Characteristics for the output voltage and input current against frequency recorded for 21-turns CNT coil used as primary winding and 12-turns coils used as secondary winding. The input voltage applied amounted to 5 V p–p. Only the data for 12 turn CNT coil are presented as the results for 12 turns copper coil were identical. d) The setup used for measurements presented in (a,b). e) The setup used for measurements presented in (c).

However, similar characteristics performed in a different arrangement of windings, that is, 21-turns CNT coil was used as a primary winding and voltage of 150 mV p–p was applied to it at various frequencies while the output voltage was measured on 12-turns copper and CNT coils used as secondary windings, Figure 4e, showed that at low frequencies the output signal decays (Figure 4b, the results were identical for both output coils therefore only the characteristics recorded for CNT coil are presented). The reduction in the transformed signal is a result of higher resistance of CNT wire compared to copper, which at low frequencies causes a large voltage drop and small electromotive force across the primary winding and thus small voltage induced on the output. This conclusion may be deduced from Equation 2. In any transformer where the $\boldsymbol{E}_1 \approx \boldsymbol{V}_1$ the supply of $\boldsymbol{V}_1$ of constant amplitude at increasing frequency will keep the constant amplitude of $\boldsymbol{E}_1$. This implies (from Equation 4 that for the increasing frequency the current will be decreasing if the inductance of the coil is assumed to be constant in this range of frequencies, which is the case in the presented experiment. In the practical transformer, high current observed at low frequencies will cause a considerable drop of voltage if the resistance of winding is high, but the effect will be considerably alleviated at high frequencies where the current is decreased. In case of the experiment presented in Figure 4b, above 200 kHz the input-output voltage ratio equals turns ratio indicating that the losses due to high resistance of primary winding become negligible. The expected decrease of input current is shown in Figure 4c which depicts the output voltage characteristics measured in the same arrangement of windings as in Figure 4b correlated with input current. It should be noted that the input voltage was set at 5 V p–p in order to obtain measurable current characteristics. The calculations performed for all the characteristics presented in Figure 4a–c using Equations 1–4 are in very good agreement with experimental data.[15] In all the calculations it was assumed that all leakage inductances L_{L1} and the resistance of the copper wire were negligible.

The next set of experiments was performed at the fixed frequency of 400 kHz, that is, within the range of frequencies where the current in the primary winding is decreased, the contribution of winding losses becomes negligible and thus voltage ratio equals turns ratio. The same winding arrangement was used i.e. 21-turns CNT coil was a primary winding and 12-turns CNT and copper coils were secondary windings. **Figure 5** shows that at frequency of 400 kHz the increase of input voltage causes a linear increase of output voltage which overlaps for both 12-turns CNT and copper coil used as secondary winding in the open circuit arrangement. The characteristics calculated theoretically from Equation 1 ($\mathbf{E}_1 \approx \boldsymbol{V}_1$ and $\boldsymbol{E}_2 \approx \boldsymbol{V}_2$) were in very good agreement with experimental plots.

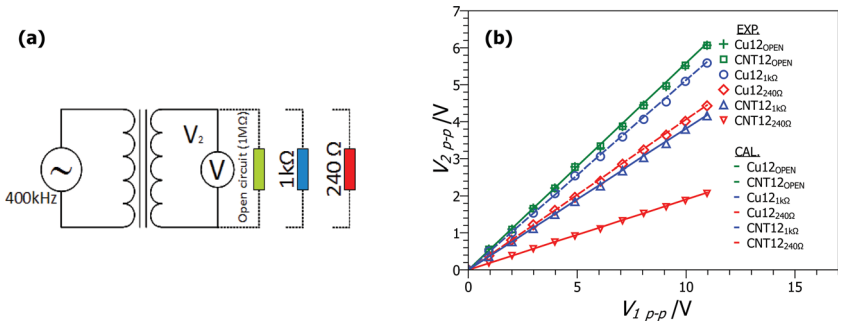

Figure 5. a) The setup used for measurements presented in (b). b) Comparison of open circuit and load characteristics which shows the output voltage measured at set frequency of 400 kHz versus a range of input voltages. 21-turns CNT coil was used as primary winding in all the measurements. In all the graphs, the data points were recorded during the experiments and the lines are the results of the theoretical calculations. In the legends Cu12 and CNT12 indicate the secondary winding used, i.e., either copper coil or CNT coil with 12 turns respectively. The subscript and colors denote the type of load used.

The same experiment performed with the loads of 1 kΩ and 240 Ω connected to the output coils also resulted in similarly linear characteristics. However, the slopes of the plots were lowered and the decrease in slope was greater for CNT winding than for copper winding which is again a result of higher resistance of the CNT coil in comparison to copper.

In the practical transformer under load the current flowing through the secondary winding induces in the core a magnetic flux which opposes the magnetic flux produced by the primary winding. The current flowing on the primary side I_1 is then a sum of the no-load current used to induce the primary magnetic flux and cover the core losses I_0, as well as of the equivalent of the current flowing on the secondary side $\boldsymbol{N_2/N_1}*\boldsymbol{I_2}$ which balances the effect of the opposing flux, that is:

$$\mathbf{I_1} = \mathbf{I_0} + \frac{N_2}{N_1}\mathbf{I_2} \tag{5}$$

Both the primary and secondary side currents are increased and the losses due to resistances and leakage inductances of the coils may become non-negligible. Then as shown in Equation 2, the losses on the primary side will cause that the $\boldsymbol{E_1} < \boldsymbol{E_1}$ and the voltage on the load will be lower than $\boldsymbol{E_2}$ (Equation 3). In case of the presented experiment, it was assumed that only the resistance of the CNT windings is non-negligible as it is considerably higher than the contributions of any leakage inductance or the resistance of copper windings. It was also assumed that the whole no-load current $\boldsymbol{I_0}$ is used to produce mutual magnetic flux.

The theoretical calculations based on Equations 1–5 performed using the results of no-load and load tests, the listed above assumptions provide very good fits to the experimental data as shown in Figure 5.[15] This implies that indeed the transformer operates in perfect agreement to the theory and the decrease in the resistance of the CNT windings will improve its performance.

Simultaneously with our bulk scale development, Mousa et al.[16] revealed microfabrication route for manufacture of a microscopic transformer with carbon nanotubes. Both, this and our work confirm that the application of CNTs in electrical machines is a very interesting area of research and that CNTs have a potential to be successfully used in electrical machines.

4. Conclusion

We tested the performance of macroscopic insulated assemblies of carbon nanotube wires by substituting them for copper windings in a standard high frequency transformer. The open circuit and load tests demonstrated that a transformer assembled with CNT wires demonstrates characteristics that are in agreement with the classical theory of electrical transformers. The transformer with CNT windings works well across a wide range of frequencies; however, the CNT wires currently produced exhibit a higher resistance than conventional copper wires, and the challenge of reducing the high resistance of the CNT windings is currently being addressed in ongoing research. Nonetheless, these early results are highly promising and demonstrate the enormous potential impact that nanotechnology can have on common everyday electrical devices.

5. Experimental Section

In this floating catalyst chemical vapour deposition process, the feedstock comprising hydrocarbons, ferrocene, sulphur compound, and hydrogen is introduced into a high temperature (1200 °C) furnace and fibres are directly spun from the aerogel of CNTs formed in the hot zone of the furnace. Before collecting the fibre, it is densified using a low boiling point solvent spray. In order to obtain CNT cords, many fibres are mechanically bundled together. The thickness and length of the CNT cord directly depends on the number of fibres bundled together and the circumference of the fibre winder used in the system, respectively. As a rough guide, to make 1 mm thick cord, about 70 fibres are bundled together.

The insulation of the cords was made using an industrially produced silicone based adhesive paste, (Dow Corning 732 multi-purpose sealant). The cord was pulled through a syringe containing the paste and left in ambient conditions (about 25 °C and average humidity of 40%) to set. The resulting coating formed a thin, transparent, flexible, and tough rubber layer on the surface of CNT cord. According to the data provided by the manufacturer, after proper curing, the sealant has a dielectric strength of 21.6 kV mm^{-1}, dielectric constant at 100 Hz/100 kHz of 2.8, dissipation factor at 100 Hz/100 kHz of 0.0015, and volume resistivity of 1.5×10^{15} Ω cm.

The E-shaped core parts, made of N87 Manganese-Zinc ferrite, were tightly joined together to ensure the minimum possible air gap in the core. The transformer was placed on a PCB board. The coil of 21-turns was made of 57 cm-long and approximately 0.35 mm thick CNT cord of 276 Ω DC resistance, whereas a 34 cm long and 0.15 mm thick CNT cord of a 374 Ω resistance was used for the winding of 12 turns. The ends of the coils were attached to BNC terminals on the same board.

A Keithley 6221 current source was used for measurements requiring a 10 mA p–p input current. The output signal was recorded on an Agilent DSO-X oscilloscope. The circuit was connected with three equally long 50 Ω coaxial cables (RG-58). In the tests where a voltage input signal was required a Gould Advance SG200 RF signal generator was used. The current measurement performed in the test presented in Figure 4c was carried out with the use of 1 Ω metal film resistor connected in series

with the primary winding and a voltmeter connected in parallel to this load (Figure 4e). For the known constant load the voltage measured across it is equal to current flowing through it. The reactance of this resistor measured in Modulab-MTS was negligible and, for example, amounted to 0.06 Ω at 400 kHz. Thus the load was assumed to be purely resistive and equal 1 Ω in all frequencies.

Supporting Information

Supporting Information is available from the Wiley Online Library or from the author.

Acknowledgements

L.K. and K.K. thank the European Research Council (under the Seventh Framework Program FP7/2007-2013, ERC grant agreement no 259061) for funding this project. A. Lekawa-Raus is grateful to Trinity College, University of Cambridge for Coutts Trotter Studentship. K. Koziol also thanks the Royal Society for financial support.

Received: July 25, 2013
Published online: September 17, 2013

[1] M. Tooley, D. Wyatt, *Aircraft Electrical and Electronic Systems: Principles, Maintenance and Operation*, Butterworth-Heinemann, Elsevier, UK **2008**.
[2] A. E. Lekawa-Raus, L. Kurzepa, X. Peng, K. K. Koziol, presented at *NT12 Thirteenth International Conference on the Science and Application of Nanotubes*, Brisbane, Australia **2012**.
[3] K. K. Koziol, J. Vilatela, A. Moisala, M. Motta, P. Cunniff, M. Sennett, A. Windle, *Science* **2007**, *318*, 1892.
[4] H. Li, K. Banerjee, in *Proceedings of IEEE International Electron Devices Meeting, IEDM 2008*, IEEE, San Francisco, USA **2008**, 1.
[5] G. Antonini, A. Orlandi, M. D'Amore, in *Proceedings of EMC Europe 2011*, York, UK **2011**, 345.
[6] W. Lu, M. Zu, J.-H. Byun, B.-S. Kim, T.-W. Chou, *Adv. Mater.* **2012**, *24*, 1805.
[7] M. Miao, *Carbon* **2011**, *49*, 3755.
[8] R. M. Sundaram, K. K. Koziol, A. H. Windle, *Adv. Mater.* **2011**, *23*, 5064.
[9] J. Vavro, J. M. Kikkawa, J. E. Fischer, *Phys. Rev. B* **2005**, *71*, 155410.
[10] Y. Zhao, J. Wei, R. Vajtai, P. M. Ajayan, E. V. Barrera, *Sci. Rep.* **2011**, *1*, 83.
[11] K. Koziol, J. Vilatela, E. Brown, L. Hao, R. Stearn, A. Windle, presented at *NT08 Ninth International Conference on the Science and Application of Nanotubes Montpellier*, France, June, **2008**.
[12] M. Burda, A. Gruszczyk, T. Kik, K. Koziol, A. Lekawa-Raus, presented at *15th International Conference on Experimental Mechanics*, Porto, Portugal, July, **2012**.
[13] Data provided by the manufacturer on the following website: http://www.dowcorning.com/applications/search/default.aspx?R = 2142EN, (accessed: October, **2011**).
[14] Data about the ferrite core provided by the manufacturer on the following website: a) http://www.farnell.com/datasheets/80891.pdf and b) http://www.epcos.com/web/generator/Web/Sections/ProductCatalog/Ferrites/Materials/PDF/PDF__N87,property = Data__en.pdf;/PDF_N87.pdf (accessed: May, **2012**).
[15] For details see Supporting Information.
[16] O. Mousa, *J. Energy Resour. Technol.* **2013**, *135*, 021201.